Int. J. Metrol. Qual. Eng. **5**, 104 (2014)
© EDP Sciences 2014
DOI: 10.1051/ijmqe/2014004

Process development for the reproducible roughness measurement of optical surfaces using white light interferometry

Johannes Liebl*, Heiko Biskup, Sebastian Draxinger, Rolf Rascher, and Christine Wünsche

Technische Hochschule Deggendorf, Labor Optical Engineering, Technologiecampus Teisnach, 94244 Teisnach, Deutschland

Received: 27 October 2013 / Accepted: 24 April 2014

Abstract. Today a wide range of instruments are available for the rapid roughness quantification of optical surfaces but especially for three dimensional measurement methods no standardized process is established. This leads to different results, even if the same specimen is tested with similar measurement devices. In order to solve this problem an exemplary process development is described in this paper. To do this firstly the term of roughness is defined as a surface deviation and then the functionality and importance of filters in roughness measurement as well as the used measurement devices are described. The following chapter defines the used materials and methods which were used during the measurement process. In the last part of this paper the results are discussed and a process assignment is suggested.

Keywords: Reproducible, roughness, measurement, white light interferometry, surface, metrology, optic, process assignment

1 Introduction – the definition of roughness

The term of roughness is described as a high frequency deviation concerning the ideal surface. Deviations from a first to a sixth order are specified in the standard DIN 4760 [1] (Tab. 1). Category one and two are straightness and waviness errors. Both of them have no reference to the roughness of a surface. They are typically measured with a tactile surface profiler. Deviations of category four and five occur mostly on polished materials. These are measured usually non tactile with interferometers, scattered light measurement devices, conoscopy or confocal microscopy. The importance of roughness increases with the frequency of the transmitted or reflected light. If wavelength of light is in the dimension of high frequent surface deviation, diffuse scattering occurs and a specific beam forming becomes impossible.

Table 1. Categories of surface deviation – DIN 4760 [1].

Surface deviation	Type of deviation	Reason of appearance
1. Category: Form deviation 	Straightness-deviation	Errors in manufacturing and work piece clamping
2. Category: Waviness 	Waves	Eccentric clamping and machine vibrations
3. Category: Roughness 	Rills	Form of the cutting edge and machine feed
4. Category: Roughness 		process of chip formation
5. Category: Roughness	Structural conditions	Chemical process

2 Roughness parameters

To describe the roughness of a surface a variety of parameters are available. Most of them were developed for surface profilers and are described in the standard DIN EN ISO 4287 [2]. With the introduction of three dimensional measuring devices the parameters were adjusted. In order to improve transparency, only the root mean square roughness S_q and the arithmetic mean roughness S_a were evaluated [3]. Due to the squaring operation the value S_q is more sensitive to measured peaks than S_a.

$$\mathrm{PV} = \text{Peak to Valley} = \max\left(z\left(x,y\right)\right) - \min(z(x,y)) \tag{1}$$

$$S_a = \frac{1}{MN}\sum_{j=1}^{N}\sum_{i=1}^{M}\left(z\left(x_j,y_i\right) - \bar{z}\right) \tag{2}$$

* Correspondence: johannes.liebl@th-deg.de

Article published by EDP Sciences

https://doi.org/10.1051/ijmqe/2014004 Published online by Cambridge University Press

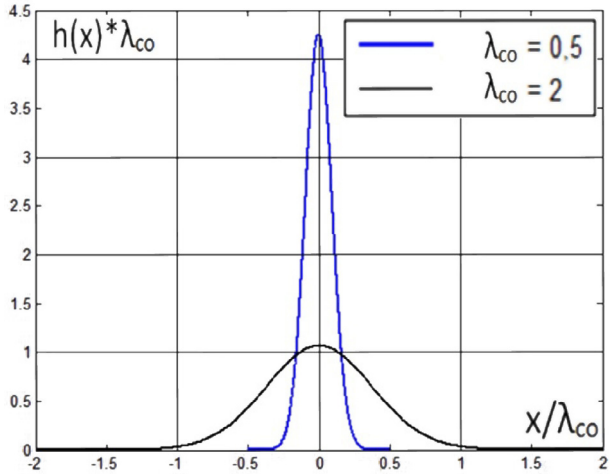


Fig. 1. Gaussian weight function for $\lambda_{co} = 0.5$ and $\lambda_{co} = 2$.

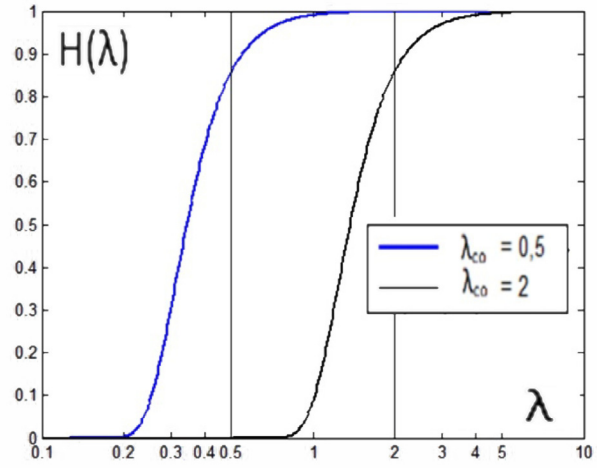


Fig. 2. Gaussian transfer function for $\lambda_{co} = 0.5$ and $\lambda_{co} = 2$.

with

$$\bar{z} = \frac{1}{MN} \sum_{j=1}^{N} \sum_{i=1}^{M} z\left(x_j, y_i\right)$$

$$S_q = \sqrt{\frac{1}{MN} \sum_{j=1}^{N} \sum_{i=1}^{M} \left(z\left(x_j, y_i\right) - \bar{z}\right)^2} \tag{3}$$

with

$$\bar{z} = \frac{1}{MN} \sum_{j=1}^{N} \sum_{i=1}^{M} z\left(x_j, y_i\right)$$

3 Measurement of roughness with high pass filters

To determine the roughness of a surface, form and waviness errors have to be subtracted from the raw measured data. This is generally done by a high pass filter. For further examinations the Gaussian filter will be used. His name derives from its bell shaped weight function. The definition of the Gaussian filter is given by the standard DIN EN ISO 11562 [4,5] and his weight function is:

$$h\left(x\right) = \frac{1}{\alpha\lambda_{co}} \exp\left[-\pi\left(\frac{x}{\alpha\lambda_{co}}\right)^2\right] \tag{4}$$

with the abscissae x, the cut off wavelength λ_{co} and the constant α:

$$\alpha = \sqrt{\frac{\ln(2)}{\pi}}. \tag{5}$$

Depending on λ_{co}, different weight functions result. As an example two graphs were created for $\lambda_{co} = 0.5$ and $\lambda_{co} = 2$ (Fig. 1).

To obtain the transfer function $H\left(\lambda\right)$ of the respective filter, a Fourier transformation of $h(x)$ is necessary. $H\left(\lambda\right)$ is given by:

$$H\left(\lambda\right) = \int_{-\infty}^{\infty} h(x) \exp\left[-i\frac{2\pi}{\lambda}x\right] dx = \exp\left[-\pi\left(\frac{\alpha\lambda_{co}}{\lambda}\right)^2\right]. \tag{6}$$

By substituting α (5) into equation (6), $H\left(\lambda\right)$ becomes:

$$H\left(\lambda\right) = \frac{1}{2}^{(\lambda_{co}/\lambda)^2}. \tag{7}$$

According to the weight functions in Figure 1, the respective transfer functions are shown in Figure 2. They indicate the cut off wavelengths at which damping starts.

The transfer function shows the typical characteristic of a low pass filter. The corresponding high pass filter is obtained by subtracting 1 an $H\left(\lambda\right)$. The filtering is executed by convolving the recorded surface profile with the function $h\left(x\right)$ (Eq. (4)). By applying a Gaussian filter waviness and form deviation can be separated from roughness (Fig. 3).

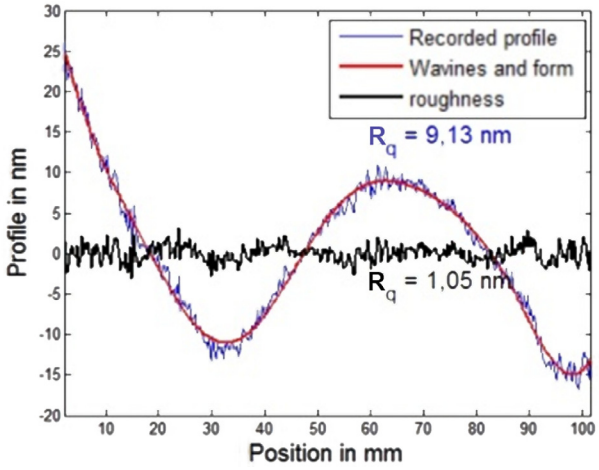


Fig. 3. Separation of waviness, form deviation and roughness – measured at TC Teisnach.

Crucial for a meaningful filtering is the choice of a correct cutoff wavelength λ_{co}. For surface profilers a standard

https://doi.org/10.1051/ijmqe/2014004 Published online by Cambridge University Press

Table 2. Cut off wavelength for high pass filtering – DIN EN SIO 4288 [6] – extended for precision optics.

S_a in nm	λ_{co} in μm
100 ... 2000	800
20 ... 100	250
6 ... 20	80
0.2 ... 6	25
<0.2	8

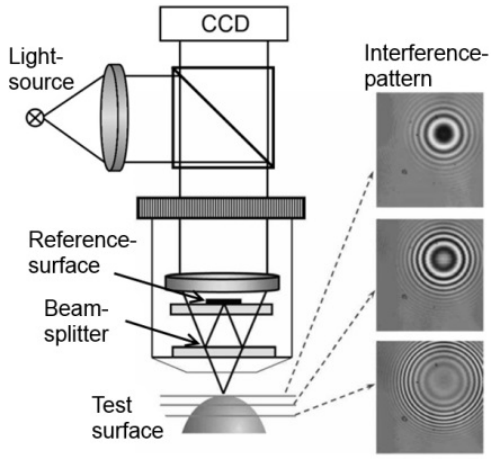


Fig. 4. Schematic construction of a white light interferometer with Mirau transmission element.

is defined in DIN EN SIO 4288 [6]. To cover the roughness requirements in precision optics, this standard has been extended periodically by two lines at the technology campus Teisnach (Tab. 2). An empirical study into meaningful cutoff wavelengths still has to be performed.

4 White light interferometry for the measurement of roughness

A withe light interferometer uses the wave nature of light, especially the interference of two beams. A light source emits white light (380–750 nm) with a low temporal and spatial coherence. In a next step the light is separated by a beam splitter. One part is reflected by the test surface, the other by an internal, highly accurate reference surface. Both of them reencounter in the beam splitter and interference. Due to the short coherence length, the interference pattern is locally strong limited (Fig. 4) [7]. The occurring stripes are evaluated by a special software which generates the three dimensional topography of the specimen.

5 Materials and methods

To measure the roughness of the test part, the Zygo NewView 7200 white light interferometer with a 20× zoom Mirau transmission element was used. This leads to a measurement area of 0.35 × 0.26 mm^2 and a lateral resolution of 0.55 microns per pixel. For evaluation the software MetroPro in version 8.3.4 was used.

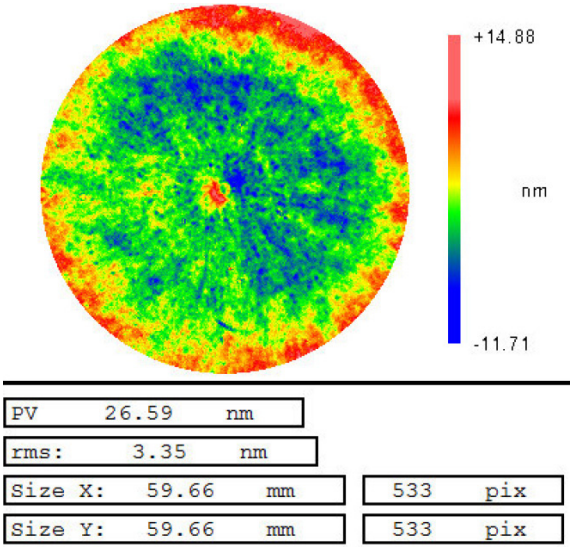


Fig. 5. Entire Specimen measured with ZygoVeriFire XP/D.

All measurements were performed at the "Technologie Campus Teisnach", a research facility of the "Labor Optical Engineering" at the Technical University of Deggendorf. A wide range of measuring instruments and machine tools are available. Because of this even complex experiments can be done in a short time. To achieve consistent results high effort was set into stable environmental conditions, especially in temperature and vibrations isolation.

Figure 5 shows the interferometric measurement of the entire specimen measured by a Zygo VeriFire XP/D. This measurement is done to show the quality of the test part. Because of the low lateral resolution of 112 microns per pixel no relation to the roughness of the surface is given. All subsequent measurements were performed with the Zygo NewView 7200 white light interferometer. The specifications of the test parts are:

- Material: N-BK7.
- Diameter: 80 mm.
- Measured diameter: 60 mm.
- Curvature: Plan.
- Thickness: 20 mm.
- PV: 27 nm.
- S_q (rms): 3.4 nm.

The polishing was done by a lever polishing machine. In this process the specimen mainly rotates and a rotational roughness distribution would be typically.

6 Averages per measurement

To reduce the statistical error of a measurement, it is necessary to perform several averages per position. It is important to find a sensible compromise between accuracy and measurement time. Two measurements were performed with an identical number of averages. Afterwards both results were subtracted from each other as shown in Figure 6. The right picture shows the difference between

https://doi.org/10.1051/ijmqe/2014004 Published online by Cambridge University Press

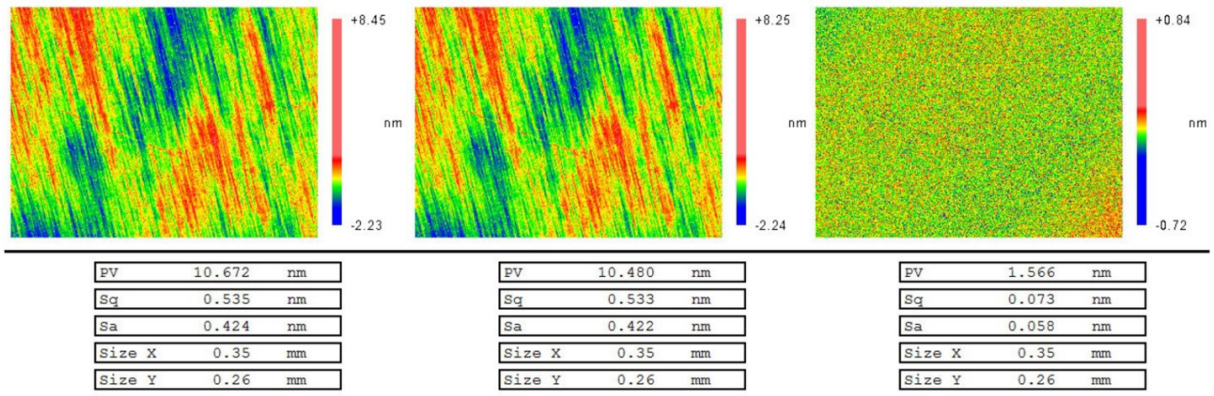


Fig. 6. Averages per measurement; left side M1; middle M2; right side M2-M1.

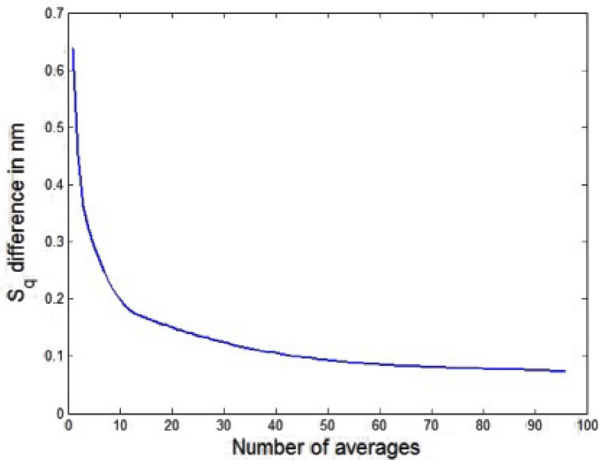


Fig. 7. Number of averages per measurement.

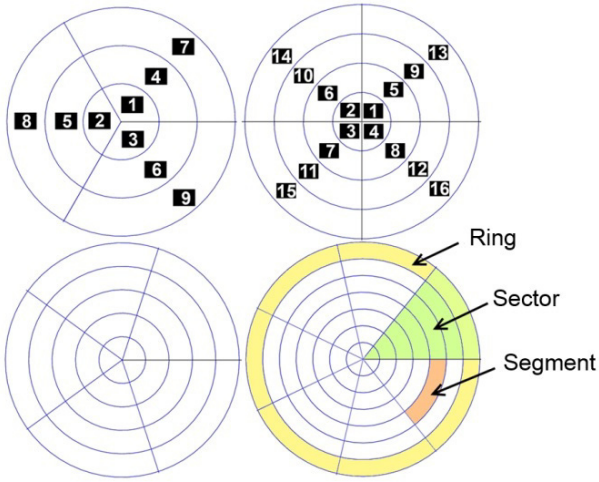


Fig. 8. Distribution of measurement points and nomenclature.

measurement one and two. Since only a statistical noise can be seen in the result it can be assumed that the number of averages was chosen sufficiently high.

Figure 7 shows the evaluation of this method. Because of this analysis, 16 averages for each individual measurement were chosen for the following measurements.

7 Roughness measurement on test part

The measurement points on the specimen were symmetrically distributed. This ensures that no ring on the test part will be ranked higher in the following averaging process (Fig. 8). With an increasing number of sectors, the number of rings was increased additionally. In the center of each segment the roughness measurement was performed. The determined value of S_q is assumed representative for each segment. Because of the small area of measurement (0.35×0.26 mm^2) in comparison to the whole surface with a diameter of 60 mm, it cannot be ensured that a representative measurement is performed. It's always an assessment of costs and benefits.

To limit the size of this publication only the four experiments in Table 3 are shown as examples. Experiment one and five contain no relevant further information.

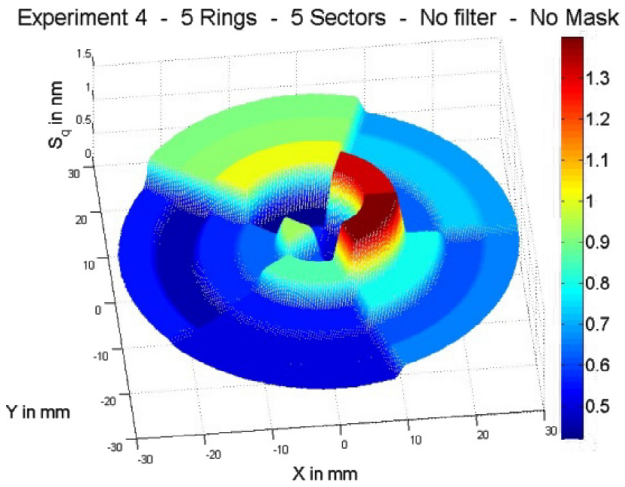


Fig. 9. Experiment 4 with no filter and no mask.

In the first experiment, just the raw data of the measurements were evaluated and neither a high-pass filtering to avoid an active form and waviness influence, nor a masking of defects was used (Fig. 9).

https://doi.org/10.1051/ijmqe/2014004 Published online by Cambridge University Press

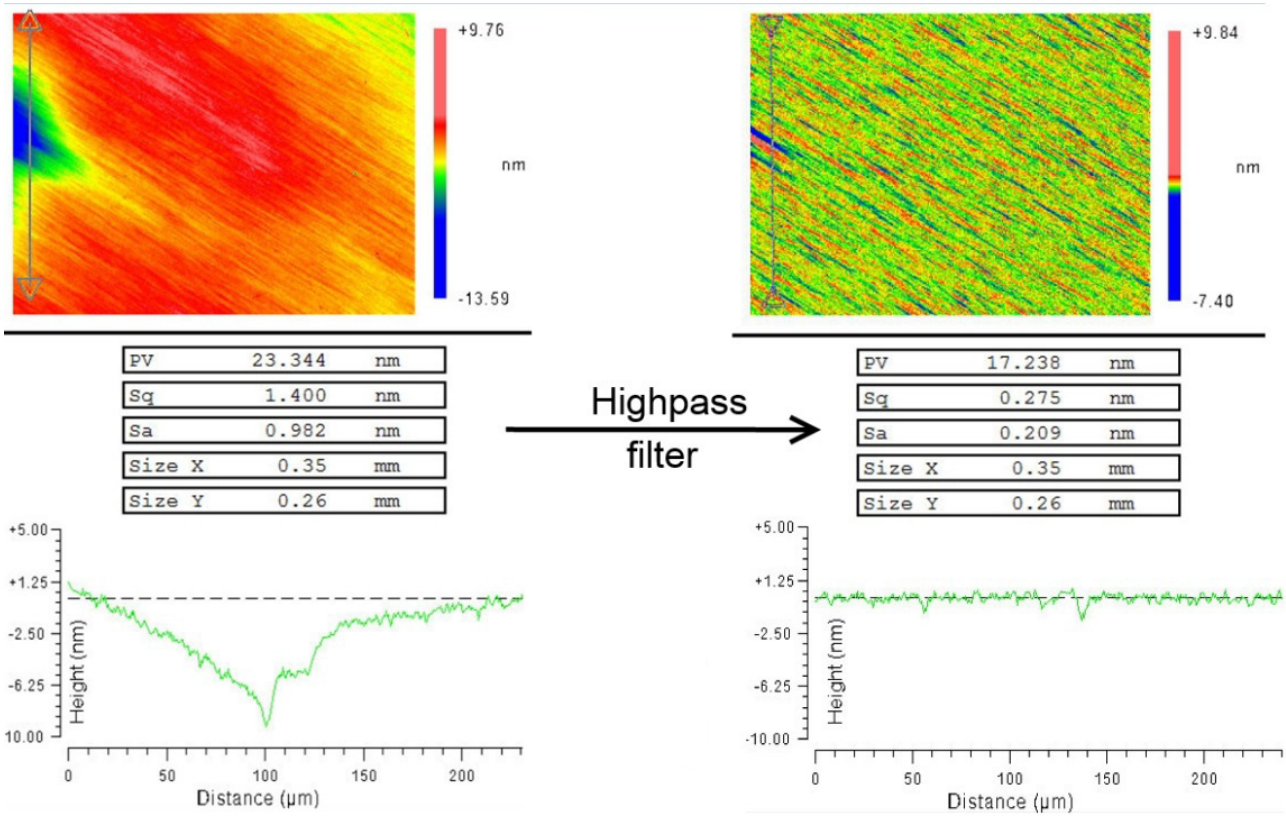


Fig. 10. High pass filtering.

Table 3. Description of the experiments.

Experiment #	Rings	Sectors	Segments
2	3	3	9
3	4	4	16
4	5	5	25
6	7	7	49

In Figure 9 one measurement of the test part is shown as an example. The segments of the roughness measurements, described in Figure 8, are still identifiable. Especially in the middle of test part some areas with high roughness values are conspicuous. These are not typical for a rotationally symmetric processing method. Therefore an error of the measurement or the following evaluation is assumed. Because of this the data of the highest roughness peak in the middle was exanimated closer (Fig. 10). Especially in the profile, the influence of form and waviness are visible. For this reason, a Gaussian high pass filter with a cut-off wavelength of 25 microns was used (selected from Tab. 2) for the following evaluations. The filtered results now only show the roughness of the respective measurement spot regardless of form and waviness errors (Fig. 10 on the right side).

By applying the high-pass filter on the individual measurements of experiment 4 a new roughness distribution results (Fig. 11).

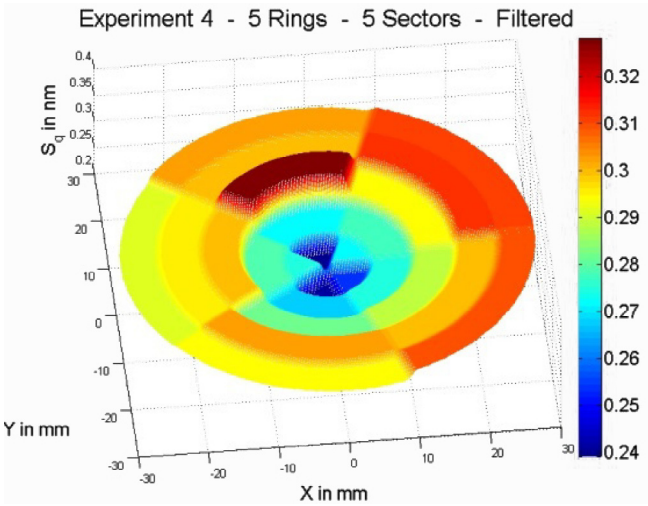
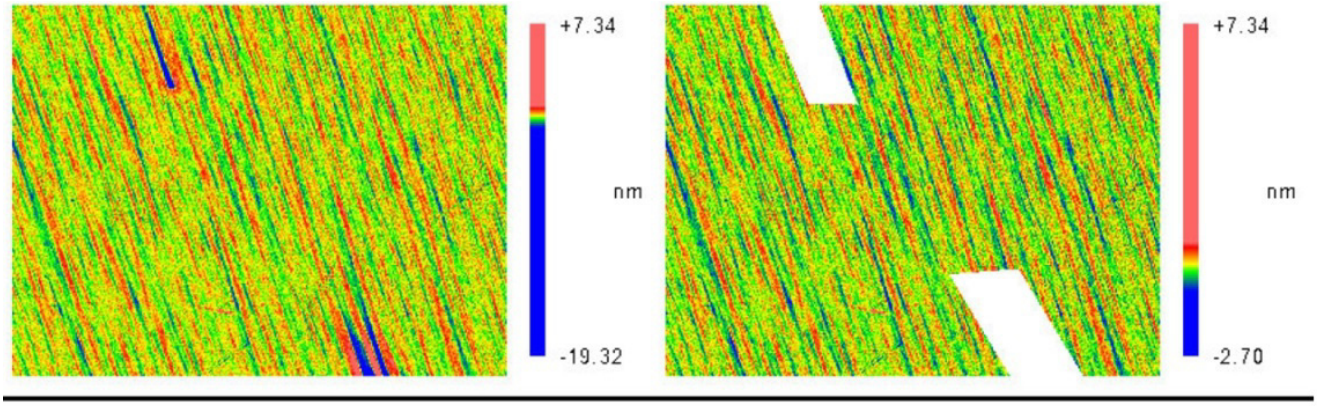


Fig. 11. Experiment 4 – high pass filtered.

By filtering experiment 4, a more significant and almost constant distribution, with low roughness values in the middle and higher values at the edge corresponding to the expectations generated by the mainly rotary polishing process, occurred. One last problem is the single peak with $S_q = 0.32$ nm. An examination of the measured data is shown in Figure 12. In the left pictur two areas with rests of form introduced by defects of the surface are visible. If these areas are masked out manually (Fig. 12 right), the

https://doi.org/10.1051/ijmqe/2014004 Published online by Cambridge University Press



PV	26.658	nm
Sq	0.328	nm
Sa	0.240	nm
Size X	0.35	mm
Size Y	0.26	mm

PV	10.046	nm
Sq	0.289	nm
Sa	0.229	nm
Size X	0.35	mm
Size Y	0.26	mm

Fig. 12. Examination of measurement data – left side with filter – right side with filter and mask.

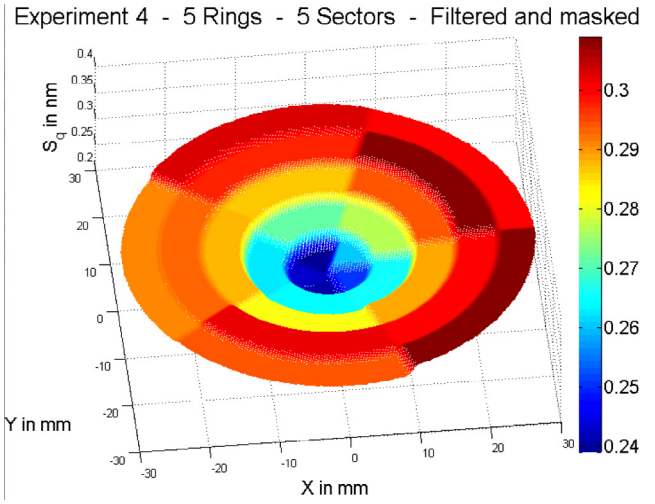


Fig. 13. Experiment 4 – high pass filtered and defects masked out.

roughness of the measurement decreases and the distribution becomes more symmetric.

The following evaluation of experiment 4 with filtering and masking of surface defects is shown in Figure 13. Discontinuities are largely eliminated and an approximately rotationally symmetric roughness distribution is obtained.

In a final step, various distributions of measurement points are compared (Fig. 14). It is aimed to obtain a representative roughness distribution with as little effort as possible.

The comparison of different measuring point distributions in Figure 14 shows no significant differences in scale or color. Thus, the distribution and number of measuring points has no significant influence on the obtained measurement results.

8 Conclusion

To ensure a conclusive distribution at least nine measurement points should be considered across the surface. It must not be forgotten that non-rotationally symmetric errors can be lost and the surface roughness is misinterpreted with less measurement points. Because of this the distribution has to match to the used polishing process. Thereby the highest possible accuracy can be achieved with minimal effort in measuring.

To measure the roughness of a sample, it is important to determine a reasonable number of averages to obtain reproducible results in the individual measuring positions. One way to achieve a reasonable number is described in Chapter 6. The number of averages could change using different measurement methods and devices.

Furthermore it can be asserted that the usage of high-pass filters is obsolete to subtract low frequency parts like form and waviness in the measured raw data.

A suitable cutoff frequency is listed in the standard DIN EN ISO 4288. For surfaces with a lower roughness the expansion in Table 2 can be used.

After filtering raw date, measurement point distribution has no significant influence on the average roughness of the surface (Fig. 15) as long as the roughness distribution is rotational symmetric.

The masking of errors only makes sense if a visual evaluation of the measuring point distribution is performed. The influence of masking on the average of the entire measurement is negligible. A very high number of defects indicate a not yet fully polished surface and a meaningful measurement of roughness is not possible with white light interferometry.

https://doi.org/10.1051/ijmqe/2014004 Published online by Cambridge University Press

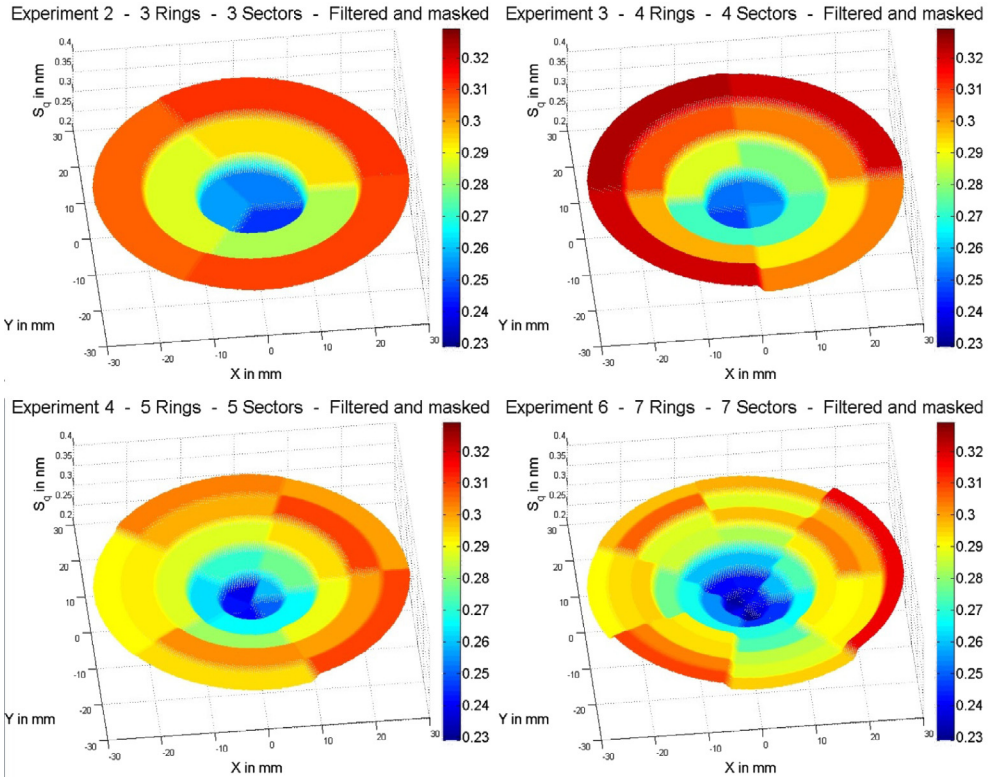


Fig. 14. Overview – different segment distribution.

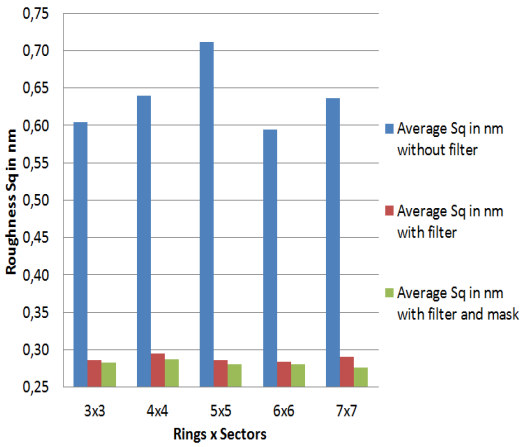


Fig. 15. Averages of roughness.

References

1. Normenausschuss Technisch Grundlagen (NATG), DIN 4760 – Gestaltabweichungen, Begriffe, Ordnungssystem (1982), p. 2
2. Normenausschuss Technisch Grundlagen (NATG), DIN 4287 – Geometrische Produktspezifikation (GPS) – Oberflächenbeschaffenheit: Tastschnittverfahren – Benennungen, Definitionen und Kenngrößen der Oberflächenbeschaffenheit (2010), p. 27
3. K.J. Stout, P.J. Sullivan, W.P. Dong, E. Mainsah, N. Luol, T. Mathia, H. Zahouani, The development of methods for the characterization of roughness in three dimensions (1993), p. 219
4. Normenausschuss Technisch Grundlagen (NATG), DIN EN ISO 16610-21 – Geometrische Produktspezifikation (GPS) – Filterung – Teil 21: Lineare Profilfilter: Gauß-Filter (2013), p. 31
5. M. Krystek, Die digitale Implementierung des Profilfilters nach DIN EN ISO 11562 (2004), pp. 4–6
6. Normenausschuss Technisch Grundlagen (NATG), DIN 4288 – Geometrische Produktspezifikation (GPS) – Oberflächenbeschaffenheit: Tastschnittverfahren-Regeln und Verfahren für die Beurteilung der Oberflächenbeschaffenheit (1998), p. 12
7. D. Malacara, *Optical Shop Testing* (2007), p. 714
8. Normenausschuss Technisch Grundlagen (NATG), DIN 4788 – Geometrische Produktspezifikation (GPS) – Oberflächenbeschaffenheit: Tastschnittverfahren-Regeln und Verfahren für die Beurteilung der Oberflächenbeschaffenheit (1998), p. 12

https://doi.org/10.1051/ijmqe/2014004 Published online by Cambridge University Press